Journal of Organometallic Chemistry, 449 (1993) 191–201

JOM 23371

A comparison of heterometallic alkoxide molecules containing copper(I) or copper(II) and zirconium

Brian A. Vaartstra, John A. Samuels, Eyal H. Barash, James D. Martin, William E. Streib, Christophe Gasser and Kenneth G. Caulton

Department of Chemistry and the Molecular Structure Center, Indiana University, Bloomington, IN 47405 (USA)

(Received August 28, 1992)

Abstract

The synthesis, characterization and structure and thermal decomposition of $ClCu^{II}Zr_2(O^iPr)_9$ (1) and $Cu^I_2Zr_2(O^iPr)_{10}$ (2) are reported. Compound 1 has a $CuZr_2(\mu_3\text{-}OR)_2(\mu_2\text{-}OR)_3$ central core, with chloride as a terminal ligand on copper. This paramagnetic Cu^{II} species is particularly interesting in that the ^1H NMR signals of those alkoxides which are μ_2- and μ_3-bridged to copper undergo paramagnetic shifts (to 8.66 and 10.41 ppm at 25°C), but those of the remaining alkoxide groups are unperturbed from the region characteristic of the $Zr_2(O^iPr)_9^-$ unit. Compound 2 consists of a $Zr_2(O^iPr)_9^-$ face-sharing bioctahedron with two μ_2-alkoxides bridging to a $Cu^I_2OR^+$ fragment giving the copper a linear two-coordinate environment. Both 1 and 2 are highly soluble in hydrocarbon solvents. TGA studies of both compounds reveal information on possible mechanisms and products of thermolysis.

1. Introduction

There is currently much interest in copper(II) alkoxides as potential precursors for superconducting copper-containing ceramics. The copper oxide lattice in these materials plays an integral role in the superconductivity. Copper alkoxides have been found to be precursors for such materials by sol/gel processes for bulk synthesis [1–4] and could be applied to CVD processes for manufacturing thin films. However, most copper(II) alkoxides are unstable [5] or insoluble and nonvolatile [6], the latter presumably because they are polymeric.

Extensive work has been conducted in heterometallic alkoxide systems [7] as a means of controlling the final ceramic product stoichiometry via the precursor. Given the large variety of metal ratios in superconductors (*i.e*, $YBa_2Cu_3O_7$, $Tl_2Ba_2Ca_2Cu_3O_{10}$, *etc.*) precursors of varying metal ratios are necessary. For example, the group of Mehrotra has reported numerous heterometallic alkoxides including the hydrocarbon-soluble $ClCu^{II}Zr_2(O^iPr)_9$ [8,9] with a 1:2 copper-heterometal ratio while we have reported [10] a $Cu^{II}_4Zr_4O_3(O^iPr)_{18}$ alkoxide cluster with a 1:1 metal ratio. In these compounds, the electrophilic zirconium serves as an *ersatz* yttrium, barium or calcium for developing synthetic principles.

We report here a further examination of Mehrotra's complex, including structural, NMR, and thermal decomposition studies. In addition, we have synthesized a new copper(I) alkoxide complex, $Cu^I_2Zr_2(O^iPr)_{10}$, which permits the examination of the effects of copper oxidation state in heterometallic alkoxides. The compound $Zr_2Cu_2(OR)_{10}$ represents a rare combination of very hard (Zr^{+4}) and very soft (Cu^+) metals, and the different bonding modes found for μ_2-OR between 2 Cu^+ and 2 Zr (or Zr + Cu) show the metals retain their character.

2. Experimental section

2.1. Materials and procedures

All manipulations were performed using standard Schlenk techniques either under an atmosphere of nitrogen or using a nitrogen-filled drybox. Toluene, pentane, hexanes, dimethoxyethane, tetrahydrofuran were dried over potassium benzophenone ketyl and distilled under nitrogen and subjected to freeze-pump-thaw cycles prior to use. The compounds $KZr_2(O^iPr)_9$

Correspondence to: Prof. K.G. Caulton.

0022-328X/93/$6.00

[11], $Zr_2(O^iPr)_8(^iPrOH)_2$ [12] and Cu(mesityl) [13] were synthesized by literature methods. Potassium hydride (Aldrich) was washed repeatedly with hexanes and dried under vacuum. Copper chloride was dried using Me_3SiCl.

2.2. Physical measurements

Hydrogen-1 and carbon-13 NMR spectra were recorded on a Nicolet NT-360 spectrometer (360 MHz and 90 MHz, respectively) and on a Bruker AM-500 spectrometer (500 MHz and 125 MHz, respectively), and referenced to residual protons in the solvent. Variable-temperature ^1H NMR spectra were recorded on a Nicolet 360 spectrometer in toluene-d_8. Temperatures were stable to within 1°C during the recording of each spectrum. Thermogravimetric analysis (TGA) was carried out on a DuPont 2100 instrument installed inside a helium-filled glove box. The TGA profile was run under a flow of helium (1 atm, 60 ml min^{-1}) at a heating rate of 10°C min^{-1} to a final temperature of 1000°C. The effluent from the TGA sample was led into a VG Micromass quadrupole mass spectrometer for identification of the volatile products. Powder X-ray diffraction studies were performed on a Scintag XDS 2000 powder diffractometer (Mo Kα).

2.3. $ClCuZr_2(O^iPr)_9$ (1)

Finely divided anhydrous copper(II) chloride (0.25 g, 1.86 mmol) and freshly sublimed $KZr_2(O^iPr)_9$ (1.40 g, 1.86 mmol) in 30 ml benzene were refluxed for 3 h, by which time all of the brown solid $CuCl_2$ had disappeared and an off-white precipitate remained. The pale green solution was allowed to cool to 25°C, then filtered to remove KCl and the solvent was removed from the filtrate under vacuum. Yield: 94%. Dissolving the benzene-soluble solid with a minimum volume (5 ml) of pentane, followed by cooling to −30°C gave medium green crystalline $ClCuZr_2(O^iPr)_9$. This crystallization (yield: 20%) leaves much of the very soluble product in solution. ^1H NMR (25°C, C_6D_6, ppm): 10.41 (br, 12H, Me), 8.66 (br, 12H, Me), 4.47 (s, 1H, CH), 4.12 (s, 4H, CH), 1.01 (s, Me), 0.96 (s, Me), 0.89 (s, Me); the last three resonances integrate to 30 hydrogens.

2.4. $Cu_2Zr_2(O^iPr)_{10}$ (2)

Solid $Zr_2(O^iPr)_8(HO^iPr)_2$ (1.00 g, 1.29 mmol) and Cu(mesityl) (0.47 g, 2.58 mmol) were combined in a Schlenk flask and suspended in 20 ml pentane at 25°C. The suspension was allowed to stir for 16 h, producing a colorless solution. Solvent was removed *in vacuo* to leave a colorless waxy solid (90% pure by NMR). Careful recrystallization from pentane produced colorless plates (20% isolated yield). ^1H NMR (benzene-d_6, 24°C): methine protons at 4.69 (sept., $J = 6.1$, 2H), 4.60 (sept., $J = 6.1$, 1H), 4.49 (mult., 6H), 4.13 (sept., $J = 5.8$, 1H); methyl protons at 1.76 (d, $J = 6.1$, 12H), 1.46 (d, $J = 6.1$, 6H), 1.36 (d, $J = 5.8$, 12H), 1.33 (d, $J = 6.1$, 12H), 1.32 (d, $J = 5.8$, 12H), 1.31 (d, $J = 5.8$, 6H). $^{13}C\{^1H\}$ NMR (benzene-d_6, 24°C): 71.3, 70.6, 70.3, 70.2, 30.4, 28.1, 27.9, 27.3, 27.2, 26.9.

2.5. X-Ray structure determination of $ClCuZr_2(O^iPr)_9$

A crystal of suitable size was cleaved from the sample in a nitrogen atmosphere glove bag. The crystal was mounted using silicone grease and was transferred to a goniostat where it was cooled to −155°C for characterization and data collection (see Table 1) [14]. A systematic search of a limited hemisphere of reciprocal space revealed intensities with 2/m Laue symmetry. Following intensity data collection ($6 < 2\theta < 45°$), the conditions $h + l = 2n$ for $h0l$ and $k = 2n$ for $0k0$ were observed which uniquely determined space group $P2_1/n$. Data processing gave a residual of 0.042 for the averaging of 1199 unique intensities which had been observed more than once. Four standards measured every 300 data showed no significant trends. No correction was made for absorption.

The structure was solved using a combination of direct methods (MULTAN78) and Fourier techniques. The four heavy atom positions were determined from an E-map. The remaining non-hydrogen atoms were

TABLE 1. Crystallographic data for compounds

$ClCuZr_2(O^iPr)_9$			
chemical formula	$C_{27}H_{63}ClCuO_9Zr_2$	space group	$P2_1/n$
a, Å	9.459(2)	T, °C	−155 °C
b, Å	24.351(4)	λ, Å	0.71069
c, Å	16.654(3)	ρ_{calcd}, g cm^{-3}	1.414
β, deg	95.06(1)	$\mu(MoK_\alpha)$, cm^{-1}	11.9
V, Å^3	3820.95	R	0.0624
Z	4	R_w	0.0603
formula weight	813.23		
$Cu_2Zr_2(O^iPr)_{10}$			
chemical formula	$C_{30}H_{70}Cu_2O_{10}Zr_2$	space group	$P\bar{1}$
a, Å	12.612(2)	T, °C	−158°C
b, Å	18.196(3)	λ, Å	0.71069
c, Å	9.830(1)	ρ_{calcd}, g cm^{-3}	1.420
α, deg	102.88(1)	μ(Mo K_α), cm^{-1}	15.155
β, deg	105.68(1)	R	0.0565
γ, deg	92.09(1)	R_w	0.0603
V, Å^3	2106.14		
Z	2		
formula weight	900.41		

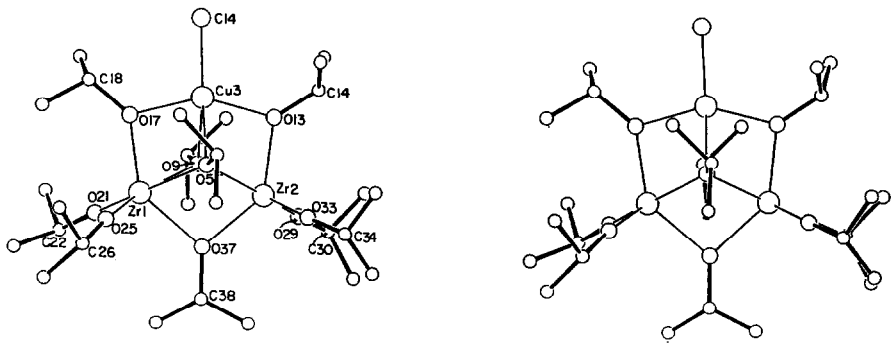

Fig. 1. Stereo ORTEP drawing of $ClCuZr_2(O^iPr)_9$, showing selected atom labelling. Hydrogen atoms have been omitted for clarity. The view is perpendicular to the $CuZr_2$ plane.

obtained from subsequent iterations of least-squares refinement and difference Fourier calculation. The isopropyl group on O(37) is disordered. The two terminal carbon atoms were modeled as four carbon half-atoms [C(39–42)]. Hydrogens were included in fixed calculated positions on all carbons except C(38–42). In the final cycles of least-squares refinement, the carbon atoms of the disordered ligand were refined with isotropic thermal parameters and all other non-hydrogens were refined with anisotropic thermal parameters. The largest peak in the final difference map was 1.5 e $Å^{-3}$ in the vicinity of the disordered ligand. All other residual peaks were less than 0.9 e $Å^{-3}$. The results of the structure determination are shown in Figs. 1 and 2 and Tables 2 and 3. Further details are available from the author as supplementary material.

2.6. *X-ray structure determination of* $Cu_2Zr_2(O^iPr)_{10}$

A single crystal fragment was cleaved from a large, colorless plate-like crystal, affixed to a glass fiber using silicon grease and transferred to the goniostat where the crystal was cooled to −158°C. All manipulations were carried out under an inert atmosphere. A systematic search of a limited hemisphere of reciprocal space yielded a set of reflections which exhibited triclinic symmetry. Subsequent refinement confirmed the choice of the space group $P\bar{1}$. Data collection [14] ($6° < 2\theta < 45°$) was undertaken as described in Table 2. The structure was solved by direct methods (SHELXS-86) and Fourier techniques. The two Zr and two Cu atoms were located in the initial E-map. The remainder of the non-hydrogen atoms were located by successive difference Fouriers. It became apparent that some of the isopropoxide carbons were somewhat disordered. This disorder was reasonably modeled by 50/50 occupancy of atoms 7/7′, 8/8′ (both on O5), 11/11′, and 12/12′ (both on O9). Hydrogen atoms were added in fixed calculated positions for the final refinement. The full matrix least-squares refinement was completed using anisotropic thermal parameters on all non-hydrogen atoms and fixed isotropic thermal parameters on the hydrogen atoms. The final difference map was essentially featureless. The largest peaks of ≤ 1 e $Å^{-3}$ were in the immediate vicinity of the metal atoms. Results of the structure determination appear in Tables 4 and 5 and Fig. 3. Additional details are available from one of the authors (KGC).

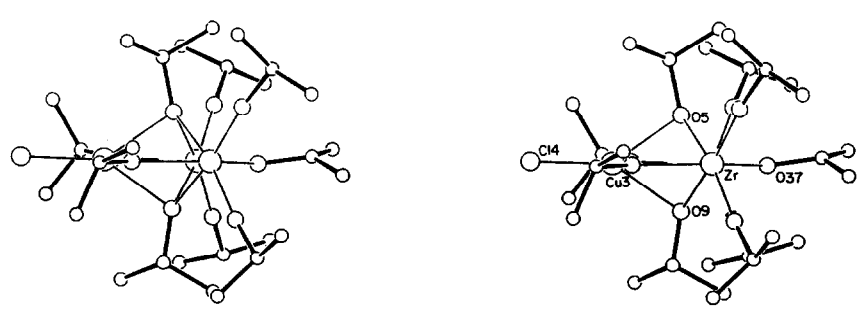

Fig. 2. Stereo ORTEP drawing of $ClCuZr_2(O^iPr)_9$ viewed down the Zr/Zr vector. Note the bending of the isopropyl groups on the μ_3-O5 and O9 towards copper.

3. Results

3.1. $ClCuZr_2(O^iPr)_9$

3.1.1. Synthesis and spectral characterization

The coupling (salt elimination) reaction between $CuCl_2$ and $KZr_2(O^iPr)_9$ has been carried out in a noncoordinating solvent in order to avoid possible solvent coordination and ligand redistribution. Given the insolubility of $CuCl_2$ in hydrocarbons, reflux temperatures facilitate the reaction. However, we have found that the yield using toluene reflux temperature is inferior to that in benzene, and thus prefer the latter. In addition, the work of Mehrotra suggests [8] addition of ^iPrOH to the reaction mixture, apparently in an attempt to solubilize $CuCl_2$. This approach must be employed with caution, since we find that too much ^iPrOH promotes the production of (insoluble) $Cu(O^iPr)_2$, KCl and $Zr_2(O^iPr)_8(^iPrOH)_2$.

TABLE 2. Fractional coordinates and isotropic thermal parameters [a] for $ClCuZr_2(O^iPr)_9$

	x	y	z	B_{iso}
Zr(1)	8035(1)	419.7(4)	7407.1(5)	13
Zr(2)	8205(1)	1771.8(4)	7234(1)	14
Cu(3)	6740(1)	1202.8(5)	8586(1)	27
Cl(4)	5633(3)	1268(1)	9666(2)	32
O(5)	8870(6)	1123(2)	8154(3)	15
C(6)	10022(10)	1193(4)	8778(5)	20
C(7)	11436(9)	1096(4)	8430(6)	23
C(8)	9789(10)	813(5)	9477(6)	31
O(9)	6515(6)	1135(2)	7272(3)	14
C(10)	5079(9)	1088(4)	6890(6)	20
C(11)	5109(11)	1073(4)	5985(6)	28
C(12)	4178(10)	1566(5)	7158(6)	28
O(13)	7153(7)	1971(3)	8258(4)	21
C(14)	6981(10)	2496(4)	8639(6)	23
C(15)	5438(12)	2636(4)	8642(7)	33
C(16)	7776(11)	2489(4)	9471(6)	29
O(17)	6879(6)	392(2)	8421(4)	18
C(18)	6287(10)	−16(4)	8926(6)	21
C(19)	6965(11)	−568(4)	8781(6)	28
C(20)	4683(10)	−31(4)	8745(6)	28
O(21)	6883(6)	−32(3)	6650(4)	21
C(22)	6171(11)	−397(4)	6100(6)	26
C(23)	6929(12)	−942(5)	6139(7)	36
C(24)	4651(12)	−465(5)	6282(7)	37
O(25)	9691(6)	−40(3)	7606(4)	20
C(26)	10945(10)	−363(4)	7653(6)	27
C(27)	11196(10)	−611(4)	8475(7)	31
C(28)	10807(13)	−795(5)	7022(9)	52
O(29)	7203(7)	2203(3)	6400(4)	21
C(30)	6556(11)	2563(4)	5815(6)	29
C(31)	5823(17)	3020(6)	6190(9)	59
C(32)	7634(19)	2778(8)	5296(11)	90
O(33)	9916(6)	2190(2)	7421(4)	21
C(34)	11093(11)	2546(4)	7506(7)	34
C(35)	11336(28)	2827(11)	6798(12)	160
C(36)	11012(20)	2908(8)	8198(14)	109
O(37)	8850(6)	1043(3)	6603(3)	19
C(38)	9796(21)	970(8)	5989(12)	83(5)
C(39)	10394(24)	1453(10)	5665(13)	35(4)
C(40)	9662(27)	472(11)	5545(15)	45(5)
C(41)	10884(26)	706(10)	5989(14)	38(5)
C(42)	8872(33)	1244(13)	5183(19)	63(7)

[a] Isotropic values for those atoms refined anisotropically are calculated using the formula given by W.C. Hamilton, *Acta Cryst.*, *12* (1959) 609; values for x, y, z have been multiplied by 10^4, and for B_{iso} by 10.

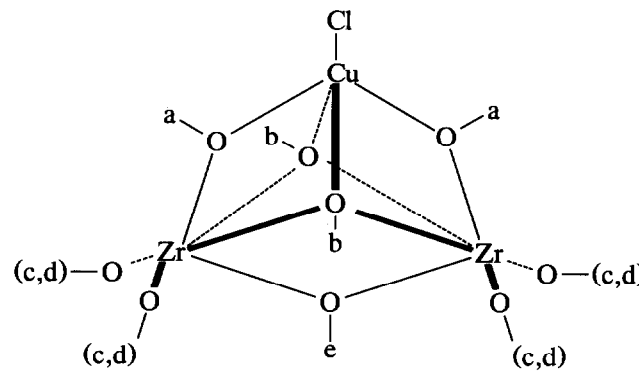

I

Structure I is consistent with the observed ^1H NMR spectrum (C_6D_6 at 25°C). The resonances are dramatically segregated into three methyl peaks (c, d and e) and two methine peaks in the region typical of isopropoxy groups in diamagnetic systems, as well as two methyl resonances (a and b) which are broad (325 Hz full width at half height) and shifted isotropically (to 8 and 10 ppm); the methine hydrogens adjacent to copper were not detected. The electron spin of Cu^{II} thus has negligible influence on those isopropoxy groups which are not directly bonded to copper.

3.1.2. Structure

The molecule is an isosceles triangle of metal atoms (Figs. 1 and 2) with (nonbonded) Zr/Cu distances of 3.07 Å and a Zr/Zr distance of 3.31 Å. The triangle is held together by three μ_2- and two μ_3-O^iPr groups. The chloride is found exclusively as a terminal ligand on Cu^{II}. Thus, the stronger π-donor O^iPr groups remain attached to the stronger Lewis acid Zr^{IV}. Formally, this molecule may be viewed as a $CuCl^+$ fragment which has a $Zr_2(O^iPr)_9^-$ unit coordinated to it in tetradentate fashion. We have recently observed this same structural type in X-ray diffraction studies on $(dme)KZr_2(O^iPr)_9$ [11] and $[(O^iPr)BaZr_2(O^iPr)_9]_2$ [15], where the formal cationic centers are $(dme)K^+$ and $(O^iPr)Ba^+$, respectively. Mehrotra has reported [16] a similar structure for $[ClCdZr_2(O^iPr)_9]_2$. Zirconium–oxygen distances increase in the sequence Zr–O_t (1.926 Å) < Zr–OCu (2.099 Å) < Zr–OZr (2.192 Å) < Zr–

TABLE 3. Selected bond distances (Å) and angles (deg) for $ClCuZr_2(O^iPr)_9$

Zr(1)–Zr(2)	3.3102(13)
Zr(1)–Cu(3)	3.0689(15)
Zr(1)–O(5)	2.221(6)
Zr(1)–O(9)	2.257(6)
Zr(1)–O(17)	2.092(6)
Zr(1)–O(21)	1.936(6)
Zr(1)–O(25)	1.931(6)
Zr(1)–O(37)	2.208(6)
Zr(2)–Cu(3)	3.0764(14)
Zr(2)–O(5)	2.251(6)
Zr(2)–O(9)	2.231(6)
Zr(2)–O(13)	2.106(6)
Zr(2)–O(29)	1.923(6)
Zr(2)–O(33)	1.914(6)
Zr(2)–O(37)	2.176(6)
Cu(3)–Cl(4)	2.1644(26)
Cu(3)–O(5)	2.207(6)
Cu(3)–O(9)	2.186(6)
Cu(3)–O(13)	1.998(6)
Cu(3)–O(17)	1.999(6)
O(13)–Zr(2)–O(29)	102.76(25)
O(13)–Zr(2)–O(33)	101.42(26)
O(13)–Zr(2)–O(37)	138.72(23)
O(29)–Zr(2)–O(33)	100.53(27)
O(29)–Zr(2)–O(37)	103.78(25)
O(33)–Zr(2)–O(37)	104.11(25)
Zr(1)–Cu(3)–Zr(2)	65.18(3)
Zr(1)–Cu(3)–Cl(4)	145.74(9)
Zr(1)–Cu(3)–O(5)	46.31(15)
Zr(1)–Cu(3)–O(9)	47.28(15)
Zr(1)–Cu(3)–O(13)	107.96(17)
Zr(1)–Cu(3)–O(17)	42.56(16)
Zr(2)–Cu(3)–Cl(4)	149.02(9)
Zr(2)–Cu(3)–O(5)	46.96(15)
Zr(2)–Cu(3)–O(9)	46.47(15)
Zr(2)–Cu(3)–O(13)	42.80(17)
Zr(2)–Cu(3)–O(17)	107.73(17)
Cl(4)–Cu(3)–O(5)	143.12(18)
Cl(4)–Cu(3)–O(9)	145.63(18)
Cl(4)–Cu(3)–O(13)	106.22(19)
Cl(4)–Cu(3)–O(17)	103.24(18)
O(5)–Cu(3)–O(9)	71.19(20)
O(5)–Cu(3)–O(13)	77.69(23)
O(5)–Cu(3)–O(17)	78.18(23)
O(9)–Cu(3)–O(13)	78.51(24)
O(9)–Cu(3)–O(17)	77.86(23)
O(13)–Cu(3)–O(17)	150.52(23)
Zr(1)–O(5)–Zr(2)	95.50(21)
Zr(1)–O(5)–Cu(3)	87.75(20)
Zr(1)–O(5)–C(6)	134.5(5)
Zr(2)–O(5)–Cu(3)	87.27(20)
Zr(2)–O(5)–C(6)	123.6(5)
Cu(3)–O(5)–C(6)	114.0(5)
Zr(1)–O(9)–Zr(2)	95.03(20)
Zr(1)–O(9)–Cu(3)	87.36(20)
Zr(1)–O(9)–C(10)	123.1(5)
Zr(2)–O(9)–Cu(3)	88.28(21)
Zr(2)–O(9)–C(10)	133.3(5)
Cu(3)–O(9)–C(10)	116.7(5)
Zr(2)–O(13)–Cu(3)	97.08(25)
Zr(2)–O(13)–C(14)	129.8(5)
Cu(3)–O(13)–C(14)	132.6(5)
Zr(1)–O(17)–Cu(3)	97.19(24)
Zr(1)–O(17)–C(18)	138.4(5)
Cu(3)–O(17)–C(18)	124.4(5)
Zr(1)–O(21)–C(22)	173.9(6)
Zr(1)–O(25)–C(26)	172.9(6)
Zr(2)–O(29)–C(30)	174.4(6)
Zr(2)–O(33)–C(34)	173.3(7)
Zr(1)–O(37)–Zr(2)	98.07(22)
Zr(1)–O(37)–C(38)	128.5(9)
Zr(2)–O(37)–C(38)	131.8(9)

μ_3O (2.240 Å). Each of the three μ_2-O^{i}Pr groups is planar at oxygen (angles sum to 358.4–360.0°), and the terminal alkoxides are nearly linear at oxygen (172.9–174.4°). Each zirconium is six-coordinate, but there are significant distortions from a regular octahedron (Fig. 1): *cis*-OZrO angles range from 69.6 to 104.1°, while the *trans* angles range from 138.3 to 164.8°. Copper is five-coordinate, and in a geometry which, while significantly distorted, resembles a trigonal bipyramid with O13 and O17 apical ($\angle$O13–Cu–O17 = 150.5°); see Fig. 1. The equatorial groups are then C14, O5 and O9, with O–Cu–Cl angles of 143.1 and 145.6 and an O5–Cu–O9 angle of only 71.2° (see Fig. 2). Associated with this very small angle are very long distances from copper to the (μ_3) alkoxide oxygens. These are 0.2 Å longer than to the (μ_2) alkoxide oxygens, while the difference of Zr–O to μ_2 and μ_3 oxygens is less than 0.1 Å. We note therefore that the μ_3-alkoxide oxygen shows nearly the same distance to copper (average value 2.197 Å) as it does to the larger zirconium atom (average value 2.240 Å). This Cu–O distance is also longer than the distance from Cu to the much larger chloride ion (2.164 Å). Thus, it may also be useful to describe the copper coordination sphere as "3 + 2", where the three more strongly bound ligands are C14, O13 and O17, with angles of 103.2 and 106.2 (both C14–Cu–O) and 150.5° (O13–Cu–O17); these three ligands approximate trigonal planar geometry. Note also (Fig. 2) that the ^{i}Pr groups of the μ_3-O^{i}Pr ligands bend towards their longest metal/oxygen bond, that to Cu. This characteristic of long μ_3-O bonds of the $Zr_2(OR)_9^-$ fragment to the hetero-metal center is not uncommon. A similar lengthening was observed in $[(OR)BaZr_2(OR)_9]_2$ where the μ_3-O-to-Ba interaction was on average 0.12 Å longer than the (μ_2-O)–Ba bond distance [15]. The zirconium/oxygen bonds in $(DME)KZr_2(OR)_9$ show a similar pattern: all the alkoxide–potassium bond lengths are approximately equal but μ_3-O-to-zirconium distances are 0.09 Å longer than the (μ_2-O)–Zr lengths [11,15]. These long bonding interactions of the μ_3 alkoxides are most likely

TABLE 4. Fractional coordinates and isotropic thermal parameters [a] for $Cu_2Zr_2(O^iPr)_{10}$

Atom	x	y	z	B_{iso}
Zr(1)	1065(1)	7797.3(4)	1030(1)	16
Zr(2)	3633(1)	7657.5(4)	1164(1)	16
Cu(3)	1115(1)	6174(1)	2086(1)	21
Cu(4)	3265(1)	6126(1)	2401(1)	21
O(5)	−25(4)	7780(3)	−804(6)	24
C(6)	−824(9)	7855(11)	−2048(14)	72
C(7)	−526(17)	8270(11)	−2887(21)	36
C(8)	−1996(13)	7735(12)	−1961(18)	29
O(9)	600(5)	8624(3)	2275(6)	23
C(10)	181(8)	9234(5)	3047(11)	33
C(11)	−645(18)	9556(12)	1738(24)	41
C(12)	−402(18)	8995(11)	3917(21)	29
O(13)	2389(4)	8420(3)	584(6)	25
C(14)	2302(7)	9119(5)	127(10)	23
C(15)	3003(16)	9729(6)	1265(14)	95
C(16)	2559(18)	9031(7)	−1226(14)	100
O(17)	2594(4)	7716(3)	2682(5)	14
C(18)	2993(7)	7991(4)	4246(9)	20
C(19)	2179(8)	7684(5)	4923(9)	30
C(20)	3168(7)	8846(5)	4714(9)	24
O(21)	4776(4)	8420(3)	2479(6)	21
C(22)	5600(7)	9029(5)	3261(10)	26
C(23)	6299(8)	8873(6)	4619(13)	46
C(24)	6269(10)	9202(6)	2282(14)	59
O(25)	4193(4)	7463(3)	−525(6)	25
C(26)	4645(10)	7341(7)	−1699(12)	51
C(27)	5274(10)	8035(8)	−1743(13)	59
C(28)	5200(13)	6659(8)	−1836(16)	77
O(29)	2049(4)	6937(3)	105(5)	16
C(30)	1586(6)	6375(5)	−1226(8)	19
C(31)	2251(8)	5696(5)	−1262(9)	30
C(32)	1532(7)	6689(5)	−2546(9)	24
O(33)	4291(4)	6747(3)	2020(6)	17
C(34)	5429(7)	6611(5)	2417(9)	22
C(35)	5843(7)	6737(5)	4056(10)	31
C(36)	5580(7)	5833(5)	1635(10)	28
O(37)	2145(5)	5532(3)	2653(6)	24
C(38)	2291(8)	5316(6)	4017(12)	41
C(39)	3239(11)	4916(9)	4372(16)	70
C(40)	1218(8)	4892(5)	3968(10)	34
O(41)	227(4)	6905(3)	1507(6)	21
C(42)	−928(7)	6824(5)	1380(10)	26
C(43)	−1506(8)	6163(6)	151(11)	38
C(44)	−1094(8)	6764(6)	2829(12)	42
C(7′)	−1517(15)	8591(11)	−1307(23)	39
C(8′)	−1430(23)	7364(16)	−2914(27)	56
C(11′)	491(17)	9987(10)	2871(19)	32
C(12′)	−975(18)	9086(12)	3045(24)	35

[a] See footnote to Table 2.

due to the loss of electron density at the oxygen with each successive bridge with consequent loss of nucleophilicity of the remaining available oxygen lone pairs.

3.1.3. Variable-temperature NMR

Given its paramagnetism, this molecule is an interesting subject for study of its isotropically shifted ^1H

TABLE 5. Selected bond distances (Å) and angles (deg) for $Cu_2Zr_2(O^iPr)_{10}$

Zr(1)–Zr(2)	3.2269(10)
Zr(1)–O(5)	1.942(5)
Zr(1)–O(9)	1.933(5)
Zr(1)–O(13)	2.178(5)
Zr(1)–O(17)	2.194(5)
Zr(1)–O(29)	2.221(5)
Zr(1)–O(41)	2.110(5)
Zr(2)–O(13)	2.177(5)
Zr(2)–O(17)	2.225(5)
Zr(2)–O(21)	1.930(5)
Zr(2)–O(25)	1.942(5)
Zr(2)–O(29)	2.206(5)
Zr(2)–O(33)	2.118(5)
Cu(3)–Cu(4)	2.6518(15)
Cu(3)–O(37)	1.836(6)
Cu(3)–O(41)	1.858(5)
Cu(4)–O(33)	1.854(5)
Cu(4)–O(37)	1.850(5)
Zr(2)–Zr(1)–O(5)	120.32(15)
Zr(2)–Zr(1)–O(9)	122.25(17)
Zr(2)–Zr(1)–O(41)	116.73(14)
O(5)–Zr(1)–O(9)	99.06(23)
O(5)–Zr(1)–O(13)	95.13(22)
O(5)–Zr(1)–O(17)	163.44(19)
O(5)–Zr(1)–O(29)	96.16(21)
O(5)–Zr(1)–O(41)	95.80(22)
O(9)–Zr(1)–O(13)	99.06(22)
O(9)–Zr(1)–O(17)	94.83(21)
O(9)–Zr(1)–O(29)	163.62(21)
O(9)–Zr(1)–O(41)	97.26(21)
O(13)–Zr(1)–O(17)	73.71(18)
O(13)–Zr(1)–O(29)	73.48(19)
O(13)–Zr(1)–O(41)	158.64(19)
O(17)–Zr(1)–O(29)	69.21(18)
O(17)–Zr(1)–O(41)	91.30(19)
O(29)–Zr(1)–O(41)	87.14(18)
Zr(1)–Zr(2)–O(21)	120.78(15)
Zr(1)–Zr(2)–O(25)	124.53(16)
Zr(1)–Zr(2)–O(33)	113.78(14)
O(13)–Zr(2)–O(17)	73.11(18)
O(13)–Zr(2)–O(21)	97.11(22)
O(13)–Zr(2)–O(25)	101.40(21)
O(13)–Zr(2)–O(29)	73.80(20)
O(13)–Zr(2)–O(33)	155.77(19)
O(17)–Zr(2)–O(21)	94.90(20)
O(17)–Zr(2)–O(25)	165.14(21)
O(17)–Zr(2)–O(29)	68.93(18)
O(17)–Zr(2)–O(33)	85.12(18)
O(21)–Zr(2)–O(25)	99.53(23)
O(21)–Zr(2)–O(29)	163.03(20)
O(21)–Zr(2)–O(33)	95.20(21)
O(25)–Zr(2)–O(29)	96.36(21)
O(25)–Zr(2)–O(33)	97.02(21)
O(29)–Zr(2)–O(33)	88.71(19)
Cu(4)–Cu(3)–O(41)	128.34(16)
O(37)–Cu(3)–O(41)	172.51(24)
Cu(3)–Cu(4)–O(33)	131.65(16)
O(33)–Cu(4)–O(37)	174.82(23)
Zr(1)–O(5)–C(6)	173.3(9)
Zr(1)–O(9)–C(10)	174.0(6)
Zr(1)–O(13)–Zr(2)	95.62(20)

TABLE 5 (continued)

Zr(1)–O(13)–C(14)	125.3(4)
Zr(2)–O(13)–C(14)	139.0(5)
Zr(1)–O(17)–Zr(2)	93.81(18)
Zr(1)–O(17)–C(18)	134.2(4)
Zr(2)–O(17)–C(18)	125.1(4)
Zr(2)–O(21)–C(22)	171.3(5)
Zr(2)–O(25)–C(26)	177.3(7)
Zr(1)–O(29)–Zr(2)	93.58(19)
Zr(1)–O(29)–C(30)	122.6(4)
Zr(2)–O(29)–C(30)	136.2(4)
Zr(2)–O(33)–Cu(4)	114.52(24)
Zr(2)–O(33)–C(34)	126.5(4)
Cu(4)–O(33)–C(34)	118.7(4)
Cu(3)–O(37)–Cu(4)	92.01(24)
Cu(3)–O(37)–C(38)	121.1(6)
Cu(4)–O(37)–C(38)	119.7(5)
Zr(1)–O(41)–Cu(3)	114.50(25)
Zr(1)–O(41)–C(42)	125.4(5)
Cu(3)–O(41)–C(42)	120.0(5)

NMR signals [17]. In fact (Fig. 4), the ^{1}H NMR chemical shifts of the two downfield iso-propyl methyl resonances ("A" and "B") show a linear dependance on T^{-1} in the temperature range (−30°C to +66°C) where they are sufficiently sharp to be measured accurately; below −30°C the lines become too broad to detect. These results (*i.e.*, simple Curie Law behavior) are consistent with a molecule with only a single $S = \frac{1}{2}$ spin state (*e.g.*, a single Cu^{II} center), and thus rule out formation in solution of any diamagnetic dimer (*e.g.*, $(\mu\text{-Cl})_2[CuZr_2(O^iPr)_9]_2$) with interacting metal centers.

The fact that significant isotropic shifts are not seen for the iso-propoxide groups not bound directly to Cu^{II} cannot be used to distinguish contact from pseudocontact mechanisms, since the diminution could be due either to ineffective spin delocalization (low A value) or to the large distance (R^{-3} very small). The d^0 configuration of Zr^{IV} makes metal/metal bond formation not viable as a mechanism for contact shift transmission of spin density. Moreover, the resistance of Zr^{IV} to undergo redox changes makes intramolecular redox, or even dative Cu → Zr bonding less likely. Overall, then a pseudocontact mechanism seems more consistent with these chemical arguments.

3.2. *Reactions of Cu(mesityl) with $Zr_2(O^iPr)_8(HO^iPr)_2$*

In order to avoid possible halide retention resulting from the use of copper(I) chloride, we chose synthesis by hydrocarbon elimination between $Zr_2(O^iPr)_8(HO^iPr)_2$ and copper(I) mesityl (CuMes). To investigate the general reactivity of these compounds with each other, initial studies were carried out in sealed NMR tubes in benzene-d_6.

3.2.1. *1:1 Reaction ratio*

We began with a reaction ratio of 1:1 CuMes to $Zr_2(O^iPr)_8(HO^iPr)_2$. At room temperature, the reaction required several hours for the pale yellow color of the copper mesityl to fade producing a colorless solution, and multiple new signals in the NMR. Focusing on the methyl region, these signals could be attributed to at least two products, the first having a broad doublet at 1.38 ppm (^3J(H–H) = 6.1 Hz), and the second having five doublets with chemical shifts of 1.76, 1.46, 1.36, 1.33, and 1.32 ppm. Also observed was a very broad septet at 4.13 ppm, approximately 0.5 ppm upfield from the other methine protons. Peaks due to mesitylene were also identified. Attempts to isolate either product from large scale 1:1 reactions under a variety of conditions only resulted in the recovery of $Zr_2(O^iPr)_8(HO^iPr)_2$.

3.2.2. *2:1 Reaction ratio*

Given the preferential crystallization of the dizirconium species, two equivalents of copper mesityl were reacted with $Zr_2(O^iPr)_8(HO^iPr)_2$ in order to consume all the alcohol present. Several hours at room temperature were required for the reaction to go to comple-

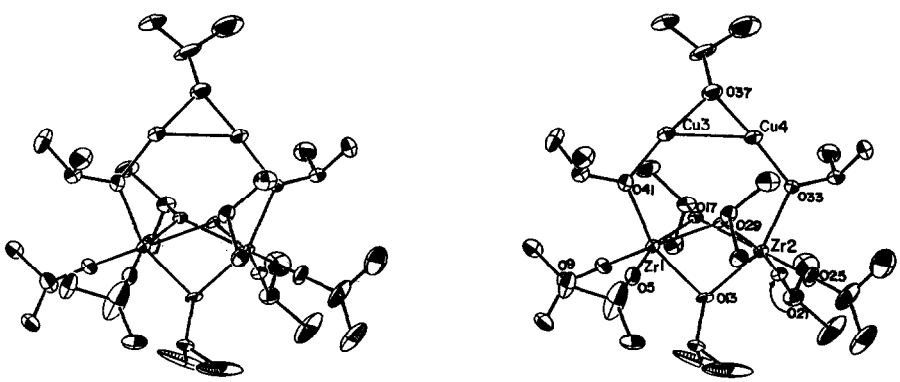

Fig. 3. Stereo ORTEP drawing of the non-hydrogen atoms of $Cu_2Zr_2(O^iPr)_{10}$, showing selected atom labelling.

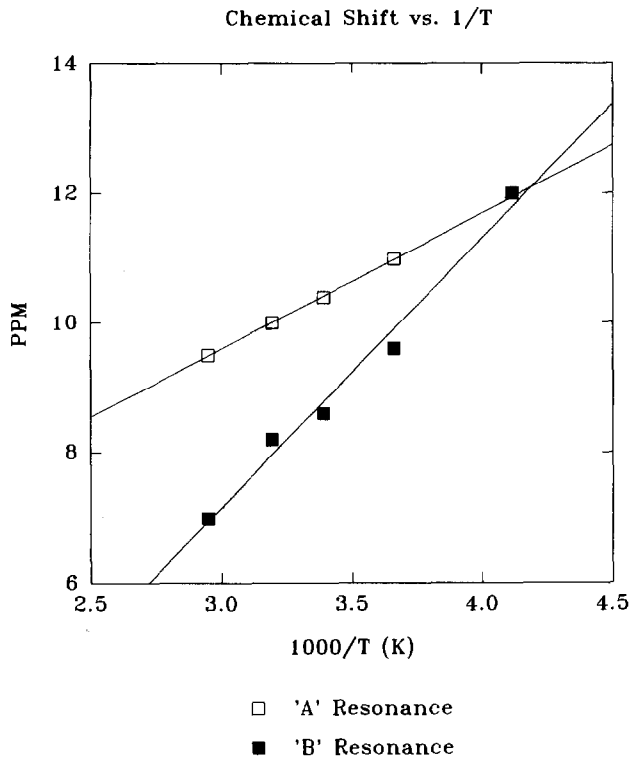

Fig. 4. Curie plot of the chemical shifts of two methyl resonances of $ClCuZr_2(O^iPr)_9$.

tion, producing a colorless solution. The ^1H NMR spectrum of the solution revealed a relatively clean spectrum with the main product having nearly the same signals as the second product reported above in the 1:1 ratio studies. The methyl region contained six doublets in an overall ratio of 12:6:12:12:12:6 while the methine region contained numerous overlapping septets between 4.4 and 4.8 ppm (with total intensity 9) and a unit intensity septet at 4.13 ppm (sharper than when observed in the 1:1 reaction). Given the reaction stoichiometry, spectral evidence, and structural precedent, structure II was tentatively assigned to this product.

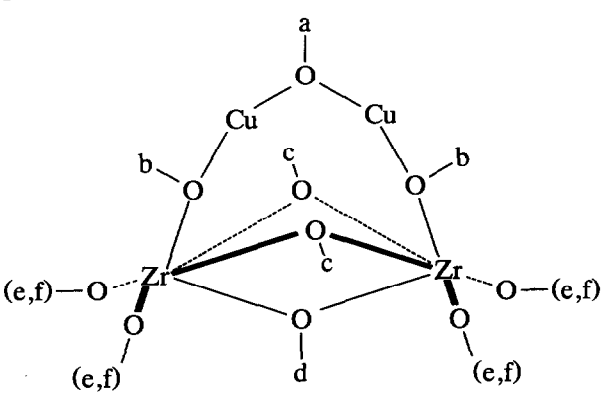

II

This structure has C_{2v} symmetry, resulting in six different chemical environments for the methyl group, as observed in the NMR. This also would seem to indicate that, at 25°C in benzene, the molecule is rigid in solution, a characteristic observed in other $MZr_2(O^iPr)_x$ complexes [11]. The NMR fails to establish whether or not alkoxides (*c*) bond to copper. Finally, the upfield alkoxide signal in the methine region was assigned to the copper bridging ligand (*a*) due to its more electron-rich environment. This alkoxide appears very labile, selectively exchanging with any free alcohol. This was confirmed by the addition of a trace amount of alcohol to an alcohol-free solution, resulting in the broadening of the signal.

3.2.3. *Excess CuMes to $Zr_2(O^iPr)_8(HO^iPr)_2$*

In order to observe the effects of excess copper mesityl, the reaction of 2.2:1 and 3:1 CuMes to $Zr_2(O^iPr)_8(HO^iPr)_2$ were performed. The reaction still required several hours at room temperature to go to completion but produced light-to-medium amber solutions and light tan precipitates with increasing CuMes concentrations. Spectra of either reaction ratio were identical to that observed for the 2:1 reaction with the exception of the increased mesitylene-to-alkoxide ratio. No new signals were observed nor was any residual copper mesityl present. Therefore either the colored species in solution was at such low concentrations to be undetectable by NMR or NMR was silent (*i.e.*, colloidal copper). The precipitate produced could account for any byproducts produced from the reaction with the copper mesityl but extensive analysis was not performed.

3.2.4. *Bulk scale synthesis of $Cu_2Zr_2(O^iPr)_{10}$ (2)*

The large-scale reaction of two equivalents of CuMes with $Zr_2(O^iPr)_8(HO^iPr)_2$ in pentane required an extended reaction time (16 h) due to the poor solubility of both reactants. Removal of the solvent from the colorless reaction solution produced the heterometallic alkoxide as a waxy colorless solid (~90% pure by NMR). Recrystallization from cold pentane resulted in a pure product as colorless plates but only in a 10–20% yield due to its extreme solubility ($KZr_2(O^iPr)_9$ is also extremely soluble in pentane).

Compound **2** was found to be highly air- and oxygen-sensitive both in solution and the solid state, producing a blue-green color. Compound **2** shows good thermal stability in a C_6D_6 solution; there is no change in its NMR signals after 20 h at 70°C. Slow decomposition does occur at temperatures greater than 80°C, producing a copper mirror and a colorless solution.

3.2.5. Structure

Single crystals of **2**, suitable for X-ray diffraction, were grown from a highly-concentrated pentane solution as colorless plates. The X-ray diffraction study shows the structure of the molecule (Fig. 3 and Table 4) to be consistent with the spectroscopic evidence. The complex contains a face-shared bioctahedral $Zr_2(O^iPr)_9^-$ unit and a bent $Cu_2(OR)^+$ fragment bound together by two bridging alkoxides. This produces a tetrametallic species where all four metals are essentially coplanar (deviation $\pm$ 0.06 Å from the least-squares plane) with each copper having a linear, two-coordinate geometry [$\angle$O–Cu–O = 172.5(2)° (Cu(3)) and 174.8(2) (Cu(4))] and each zirconium surrounded by six alkoxides in a distorted octahedron. The combination of these geometries produced an eight-membered ring (the eighth member being O(13)) in a fashion not too dissimilar from the planar $Cu_4(O^tBu)_4$ [18] structure. This overall configuration results in a relatively short Cu/Cu separation of 2.652(2) Å.

The alkoxide geometry varies greatly throughout the structure. The terminal alkoxides on the zirconium centers are nearly linear (> 171.3°) and O(13), O(33), and O(41) of the bridging alkoxides are planar (angles sum to > 359.7°). This is consistent with a highly ionic environment for these ligands, where the oxygen behaves as an isotropic point charge [19]. Alternatively, π-donation from these oxygens to zirconium may prevent the lone pairs from being stereochemically active. In contrast, the alkoxide group bridging the two less-electrophilic Cu^I centers is pyramidal (angles at O(37) sum to 332.8°), consistent with higher covalent bond character and the presence of a stereochemically-active lone pair (similar to $(CuO^tBu)_4$). It is for this reason that this alkoxide exchanges most readily with free alcohol. The last two μ-O^iPr groups seem to lie between these two extremes with the oxygen only slightly distorted from planarity; angles sum to 352.4° for O(17) and to 353.1° for O(29). This departure from planarity may be due to interaction with the coppers, either steric or electronic (bonding) in nature. In either case, the interactions are likely to be weak due to the long distances involved (> 3.020 Å).

The bond lengths are in the order Cu–O(37) (1.843 Å) < Cu–O (Zr) (1.856 Å) < Zr–O (terminal) (1.937 Å) < Zr–O(Cu) (2.115 Å) < Zr–O(13) (Zr) (2.178 Å) < Zr–O(17,29) (Zr) (2.212 Å). The fact that the Zr–O distances to the oxygens bent towards the two coppers are longer than those to O(13) reinforces the idea that O(17) and O(29) feel some influence of the copper. It is also noteworthy that the Cu/O distances to O(37) are of the same magnitude as to the oxygens which bridge to the zirconiums [O(33), O(41)], even though the ligands are in substantially different environments.

3.2.6. TGA

Thermogravimetric analysis of $ClCuZr_2(O^iPr)_9$ reveals that, in the solid state, this compound undergoes three quite abrupt weight losses. These begin at quite low temperature. The first is a very steep step which begins at 165°C. The 8% weight loss corresponds to 7.3% calculated for loss of one O^iPr group. Since this process is accompanied by a significant color change away from the light green of Cu^{II} to a reddish hue, we propose that there has been reduction to Cu^I. Both ^iPrOH and acetone are detected by coupled TGA-mass spectrometric analysis. This process is followed immediately (*i.e.*, there is no horizontal "plateau" of constant mass) by a second step of mass decrease totalling an additional 79%. This begins at 175°C and is complete by 260°C. This weight loss corresponds to loss of $Zr_2(O^iPr)_8$ (theory: 81%), a material shown independently [15] to sublime under these conditions. The remaining 13% of the original mass, which would correspond to CuCl (theory: 12.1%), undergoes a slow 5% weight loss from 280°C to 450°C producing a final mass of 8%. This value is consistent with the product being copper metal (theory: 7.8%), which is confirmed by powder X-ray diffraction. No further weight loss is observed up to a final temperature of 1000°C.

TGA of $Cu_2Zr_2(O^iPr)_{10}$ reveals that this species also undergoes rapid thermal decomposition at low temperatures, this time in a two-step process. The first step results in a 24% loss of mass with the onset occurring at 140°C, 25°C less than compound **1**. This step is too large for that expected (13.1%) for a $Cu^I \rightarrow Cu^0$ transformation by the corresponding loss of two isopropoxides. However, it is too small to involve extensive decomposition of the zirconium alkoxide portion of the molecule. This step is immediately followed by a second, more dramatic step in which approximately 55% of the mass is lost. The final average mass of 21% is obtained by 310°C and no further mass loss is observed up to 1000°C. Powder X-ray diffraction reveals the crystalline product to consist of copper metal with trace amounts of ZrO_2; the presence of ZrO_2 is consistent with the final mass being too high for pure copper (theory: 14.1%) but too low for a copper zirconium oxide (minimum theory: 41.4% for $Cu_2^0Zr_2O_4$). Attempts to obtain mechanistic information from the TGA study of **2** are frustrated by two factors. The first is that, since the first and second step seem to occur nearly concurrently, the first weight loss values obtained will contain an unknown contribution from the second step, resulting in erroneously high values. In addition, the final weight was unusually variable, with a deviation of nearly 5%. This would imply that the sample either did not cleanly decompose or was inhomogenously contaminated with an impurity. This is

supported by the presence of only trace amounts of ZrO_2 in the final powder X-ray diffraction.

4. Discussion

The formation of a heterometallic alkoxide by salt elimination between $CuCl_2$ and $KZr_2(O^iPr)_9$ is perhaps understandable in that $Zr_2(O^iPr)_9^-$ should be considered a multidentate sequestering agent and KCl precipitation may provide a thermodynamic assist. The high-temperature ^1H NMR data show that the resulting structure is stereochemically rigid: no alkoxide site-exchange is observed at 66°C. Thus the T^{-1} chemical shift dependance shows that the line broadening observed at 25°C is due primarily to paramagnetism, not site exchange. This is consistent with the fact that $Cu_2Zr_2(O^iPr)_{10}$ is also stereochemically rigid at 25°C.

It is worth noting that molecules of formula $L_nEZr_2(O^iPr)_9$ are now known where the electrophile E^{q+} has ionic radii varying from 0.74 Å (Cu^{2+}) to 1.52 Å (K^+), yet their interaction with $Zr_2(O^iPr)_9^-$ remains quite similar (*e.g.*, binding to four isopropoxide oxygens). The only exception is $(^iPrOH)LiZr_2(O^iPr)_9$, which has structure III [11]. Since the ionic radius of Li^+ is 0.73 Å, the structural difference between III (which was proposed [8,9] for $ClCuZr_2(O^iPr)_9$ [8]) and that actually observed for $ClCuZr_2(O^iPr)_9$ must originate in electronic, not steric factors: copper d orbitals permit a higher coordination number than that available via the s and p orbitals of Li^+ [20*].

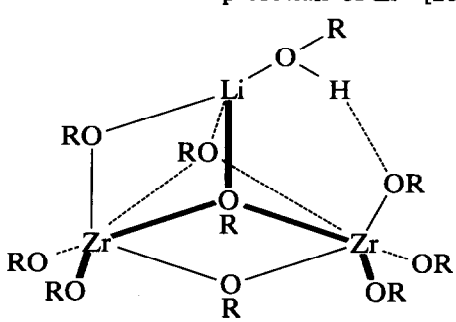

III

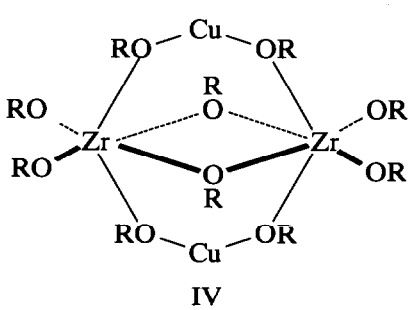

IV

* Reference number with an asterisk indicates a note in the list of references.

Although our synthetic method for the Cu^I heterometallic compound is a formal replacement of two H^+ by two Cu^+, the structure of the resulting product does not have the copper centers where the protons were (as in IV). The reasons for this dramatic change in structure are twofold. The first is the coordination geometry in IV, which would require either the copper to be in a bent two-coordinate environment or the alkoxides to bridge at a very acute angle; both are unfavorable. The second contributing factor is the potentially stabilizing copper–copper interaction present in **2**. The planar nature of the observed structure of $Cu_2Zr_2(O^iPr)_{10}$ represents an initial stage of growth of a metal oxide layer structure. Both of the structures reported here show the versatility of the $Zr_2(OR)_9^-$ unit as a structural component of heterobimetallic species. Such versatility is particularly true since the Cu^I species is the first case where two of the alkoxides bridging in the $Zr_2(OR)_9^-$ unit do *not* bind to the heterometal. This implies that such binding is dictated by the requirements of the heterometal itself. The similarities between **1** and **2** are shown in their thermolysis. Both species undergo thermal decomposition at approximately the same temperature with the first step apparently involving redox at the copper centers followed by the elimination of the resulting neutral $Zr_2(O^iPr)_8$ unit. In the case of **1**, the slightly higher temperature of decomposition is likely to be due to the stability effect of the chloride ion, but in spite of this, copper metal remains the final product.

Since both species undergo roughly the same decomposition process, it appears that, for this type of system, the initial oxidation state of the copper has little mechanistic effect. However, the fact that in both compounds, the copper is reduced at all seems to emphasize that the mobile β-hydrogens of the isopropoxy groups create a reducing environment in these heterometallic alkoxide compounds (eqn. (1)).

$$XCu^nOCHMe_2 \xrightarrow{\Delta} XCu^{n-1} + \tfrac{1}{2}H_2 + OCMe_2 \qquad (1)$$

Future work on the effects of the alkoxy ligands on the thermal decomposition of copper-containing heterometallic compounds is planned.

5. Conclusions

It has been shown that copper-containing heterometallic alkoxides can be synthesized via salt elimination or protonolysis chemistry in a variety of metal ratios and oxidation states. TGA studies have shown that decomposition products of these copper-zirconium alkoxides may be more dependent on the alkoxide ligand than the copper oxidation state.

6. Supplementary material available

Full crystallographic details, anisotropic thermal parameters and observed and calculated structure factors on two compounds are available from one of us (KGC).

Acknowledgment

This work was supported by the Department of Energy. We thank Scott Horn for skilled technical assistance and Cecilia Zechmann and Roger Kuhlman for stimulating discussions.

References and notes

1 N. N. Sauer, E. Garcia, K. V. Salazar, R. R. Ryan and J. A. Martin, *J. Am. Chem. Soc., 112* (1990) 1524.
2 C. P. Love, C. C. Torardi and C. J. Page, *Inorg. Chem., 31* (1992) 1784.
3 S. C. Goel, K. S. Kramer, P. C. Gibbons and W. E. Buhro, *Inorg. Chem., 28* (1989) 3619.
4 H. S. Horowitz, S. J. McLain, A. W. Sleight, J. D. Druliner, P. L. Gai, M. J. VanKavelaar, J. L. Wagner, B. D. Biggs and S. J. Poon, *Science, 243* (1989) 66.
5 G. M. Whitesides, J. S. Sadowski and J. Lilburn, *J. Am. Chem. Soc., 96* (1974) 2829.
6 S. C. Goel, K. S. Kramer, M. Y. Chiang and W. E. Buhro, *Polyhedron, 9* (1990) 611. A. P. Purdy and C. F. George, *Inorg. Chem., 30* (1991) 1969; A. P. Purdy, C. F. George and J. H. Callahan, *Inorg. Chem., 30* (1991) 2812; M. E. Gross, *J. Electrochem. Soc., 138* (1991) 2422.
7 K. G. Caulton and L. G. Hubert-Pfalzgraf, *Chem. Revs., 90* (1990) 969.
8 R. K. Dubey, A. Singh and R. C. Mehrotra, *J. Organomet. Chem., 341* (1988) 569.
9 R. K. Dubey, A. Singh and R. C. Mehrotra, *Polyhedron, 6* (1987) 427.
10 J. A. Samuels, B. A. Vaartstra, J. C. Huffman, K. L. Trojan, W. A. Hatfield and K. G. Caulton, *J. Am. Chem. Soc., 112* (1990) 9623.
11 B. A. Vaartstra, J. C. Huffman, W. E. Streib and K. G Caulton, *J. Chem. Soc., Chem. Commun.*, (1990) 1750; B. A. Vaartstra, W. E. Streib and K. G. Caulton, *J. Am. Chem. Soc., 112* (1990) 8593.
12 B. A. Vaartstra, J. C. Huffman, P. S. Gradeff, L. G. Hubert-Pfalzgraf, J. C Daran, S. Parraud, K. Yunlu and K. G. Caulton, *Inorg. Chem., 29* (1990) 3126.
13 T. Tsuda, K. Watanabe, K. Miyata, H. Yamamoto and T. Saegusa, *Inorg. Chem., 20* (1981) 2728.
14 J. C. Huffman, L. N. Lewis and K. G. Caulton, *Inorg. Chem., 19* (1980) 2755.
15 B. A. Vaartstra, J. C. Huffman, W. E. Streib and K. G. Caulton, *Inorg. Chem., 30* (1991) 3068.
16 S. Sogani, A. Singh, R. Bohra, R. C. Mehrotra and M. Nottemeyer, *J. Chem. Soc., Chem. Commun.*, (1991) 738.
17 I. Bertini and C. Luchinat, *NMR of Paramagnetic Molecules in Biological Systems*, Benjamin Cummings, Menlo Park, CA, 1986, Chap. 2.
18 T. Greiser and E. Weiss, *Chem. Ber., 109* (1976) 3142.
19 R. H. Cayton, M. H. Chisholm. E. R. Davidson, V. F. DiStasi, P. Du and J. C. Huffman, *Inorg. Chem., 30* (1991) 1020.
20 A referee has disagreed, arguing that lithium coordination numbers higher than 4 are "well known". S/he feels that "...the hydrogen bonding interaction in the lithium complex is sufficient to explain the different structure adopted by this species." We agree, but feel that the *reason* for alcohol coordination, is that if lithium (devoid of terminal ligands) replaced Cu in the structure of **1**, the geometry at lithium (all ligands in less than one hemisphere) is unsuitable.